Atmos. Chem. Phys., 13, 5567–5585, 2013
www.atmos-chem-phys.net/13/5567/2013/
doi:10.5194/acp-13-5567-2013

Atmospheric Chemistry and Physics Open Access

On the "well-mixed" assumption and numerical 2-D tracing of atmospheric moisture

H. F. Goessling[1,2,*] **and C. H. Reick**[1]

[1]Max Planck Institute for Meteorology, Hamburg, Germany
[2]International Max Planck Research School on Earth System Modelling, Hamburg, Germany
[*]now at: Alfred Wegener Institute, Helmholtz Centre for Polar and Marine Research, Bremerhaven, Germany

Correspondence to: H. F. Goessling (helge.goessling@awi.de)

Received: 15 September 2012 – Published in Atmos. Chem. Phys. Discuss.: 22 November 2012
Revised: 12 April 2013 – Accepted: 3 May 2013 – Published: 6 June 2013

Abstract. Atmospheric water vapour tracers (WVTs) are an elegant tool to determine source–sink relations of moisture "online" in atmospheric general circulation models (AGCMs). However, it is sometimes desirable to establish such relations "offline" based on already existing atmospheric data (e.g. reanalysis data). One simple and frequently applied offline method is 2-D moisture tracing. It makes use of the "well-mixed" assumption, which allows for treating the vertical dimension integratively. Here we scrutinise the "well-mixed" assumption and 2-D moisture tracing by means of analytical considerations in combination with AGCM-WVT simulations.

We find that vertically well-mixed conditions are seldom met. Due to the presence of vertical inhomogeneities, 2-D moisture tracing (i) neglects a significant degree of fast-recycling, and (ii) results in erroneous advection where the direction of the horizontal winds varies vertically. The latter is not so much the case in the extratropics, but in the tropics this can lead to large errors. For example, computed by 2-D moisture tracing, the fraction of precipitation in the western Sahel that originates from beyond the Sahara is $\sim 40\,\%$, whereas the fraction that originates from the tropical and Southern Atlantic is only $\sim 4\,\%$. According to full (i.e. 3-D) moisture tracing, however, both regions contribute roughly equally, showing that the errors introduced by the 2-D approximation can be substantial.

1 Introduction

Source–sink relations of atmospheric moisture characterise the Earth's hydrological cycle. They have been used, for example, to investigate the cause of extreme precipitation events (e.g. Sodemann et al., 2009) and to estimate to what extent precipitation is sustained by continental moisture recycling (e.g. van der Ent et al., 2010). Source–sink relations of atmospheric moisture are considered to contain information on how strongly precipitation somewhere is causally linked to evaporation elsewhere, though the conclusiveness of source–sink relations to establish causalities is not beyond controversy (Goessling and Reick, 2011). Nevertheless, knowledge about the paths moisture takes in the atmosphere is believed to be associated with at least some predictive skill, for example regarding the impact potential land-use changes may have on precipitation patterns.

By measuring the ratios of stable water isotopes in precipitation (e.g. Dansgaard, 1964; Salati et al., 1979), one can retrieve only vague information on where the water has evaporated; the few degrees of freedom that are associated with the stable-isotope composition do not allow for the determination of a reasonably resolved spatial pattern of the evaporative sources. To determine the latter, one has to recur to numerical tracing of moisture, which can be done either online within an atmospheric general circulation model (AGCM), or offline, i.e. a posteriori, using suitable data on evaporation, precipitation, and atmospheric transport.

Online moisture tracing was first applied by Koster et al. (1986) and Joussaume et al. (1986). In this context, Bosilovich (2002) coined the term passive water vapour

tracers (WVTs; the terminology is slightly misleading as not only gaseous water but all states of atmospheric water are meant). Here, *passive* means that the prognostic variables of the AGCM are not affected by the WVTs (see also Bosilovich and Schubert, 2002; Bosilovich et al., 2002). Online tracing offers the advantage that all state variables required for the tracing are available at the unreduced spatio-temporal resolution of the AGCM, allowing for high accuracy of the tracing. Disadvantages of online tracing are that (i) AGCMs not constrained by data assimilation cannot reproduce particular real-world situations but only reflect the Earth's long-term climate, including inevitable biases; and that (ii) to determine the fate of the moisture evaporated from each predefined set of source regions, one has to run the whole computationally expensive AGCM.

By contrast, offline moisture tracing is computationally less expensive and can be applied to different kinds of data, including reanalyses that arguably constitute the best guess of the evolution of the global atmospheric state during recent decades. While the generation of reanalyses involves AGCMs, the stored output data typically neither contain all atmospheric state variables needed to perform a full 3-D tracing comparable to online tracing, nor is their temporal resolution as high as the one at which online tracing is performed (i.e. the temporal resolution of AGCMs). While the large-scale flow field is usually sufficiently characterised by reanalysis data, processes that cause vertical redistribution of moisture in addition to the explicitly represented (large-scale) part are usually not sufficiently represented in the data. For full moisture tracing, data typically lack information on turbulent transfer coefficients and vertically resolved precipitation fluxes. It may be noted here that numerical diffusion is another (artificial) process of redistribution associated with numerical tracing, be it online or offline.

Several offline moisture tracing techniques have been developed that cope with the limitations of reanalysis-like data. Among these are relatively complex approaches like the Lagrangian particle dispersion method (e.g. Stohl and James, 2004) and the quasi-isentropic back-trajectory method (e.g. Dirmeyer and Brubaker, 1999), but also the conceptually simpler approach of 2-D moisture tracing (Yoshimura et al., 2004; van der Ent et al., 2010; van der Ent and Savenije, 2011; Goessling and Reick, 2011; Keys et al., 2012). In the latter case, the atmospheric fields are integrated vertically before the tracing is then performed in the horizontal dimensions only, either forward or backward in time. For a comprehensive overview on moisture tracing methods, we refer the reader to Gimeno et al. (2012).

2-D moisture tracing has been applied to estimate continental precipitation recycling ratios (i.e. the (spatially resolved) fraction of precipitation that stems from continental evaporation; Yoshimura et al., 2004; van der Ent et al., 2010; Goessling and Reick, 2011) and continental evaporation recycling ratios (i.e. the (spatially resolved) fraction of evaporation that precipitates on land; van der Ent et al., 2010), but has also been used to determine source–sink relations at geographically smaller scales. Recently, Keys et al. (2012) used 2-D moisture tracing to determine what they call the precipitationsheds of certain regions supposed to be particularly vulnerable to changes in precipitation. For the western Sahel, Keys et al. (2012) found that the Mediterranean and adjacent regions contribute substantially to the growing-season precipitation of the region, while relatively small amounts of moisture are advected from the tropical Atlantic Ocean (Fig. 3 in Keys et al., 2012).

However, we have argued earlier (Goessling and Reick, 2011) that 2-D moisture tracing may produce large errors, particularly in tropical and subtropical Western Africa because of the meteorological situation prevailing there in summer: while in the monsoonal layer below 750 hPa moisture is advected from the tropical Atlantic, the African easterly jet above 750 hPa carries moisture from the east and the north. In this study we therefore put one focus on the western Sahel.

The theoretical basis of 2-D moisture tracing is the so-called "well-mixed" assumption: the fractions of moisture stemming from different evaporative source regions in total atmospheric moisture are assumed to be independent of height. The "well-mixed" assumption has a long history and was first used in the context of simple, regionally applied recycling models (e.g. Budyko, 1974; Brubaker et al., 1993; Eltahir and Bras, 1994). These recycling models included further simplifications that were associated with averaging over other dimensions. Put in context to these simpler recycling models, 2-D moisture tracing is the least simplifying method that still invokes the "well-mixed" assumption for the vertical dimension – all other dimensions (the horizontal space dimensions and the time dimension) are explicitly resolved. It is worth mentioning that there are also attempts to relax the "well-mixed" assumption while keeping simplifications regarding the other dimensions (e.g. Burde, 2006; Fitzmaurice, 2007).

In view of the wide use of 2-D moisture tracing, here we analyse the conditions for its validity. Partial results to this question have been obtained by Bosilovich (2002). To investigate the validity of the "well-mixed" assumption, he traced moisture from different source regions located in North America using an AGCM equipped with WVTs. Bosilovich (2002) found that the moisture stemming from these regions tends to be inhomogeneously distributed vertically, with moisture of local origin being enriched in the lower levels. In our study we further investigate the validity of the "well-mixed" assumption using basically the same methodology as Bosilovich (2002). In addition, we quantify the errors that arise from the 2-D approximation by comparing source–sink relations of atmospheric moisture as determined with 2-D and 3-D moisture tracing.

The paper is structured as follows. In Sect. 2 we set forth the theoretical basis of the 2-D approximation and show that 2-D tracing is exact under vertically well-mixed conditions. In Sect. 3 we briefly describe the AGCM we use and our

WVT implementation. In Sect. 4 we inspect characteristics of the atmosphere that determine whether the atmosphere is well-mixed or not. In Sect. 5 we investigate to what extent the "well-mixed" assumption holds according to our simulations. In Sect. 6 we compare results obtained by 2-D moisture tracing with results obtained by 3-D moisture tracing. Finally, we summarise our findings and draw conclusions in Sect. 7. A detailed description of the WVT implementation and a comparison of different 3-D tracing variants can be found in Appendices A and B.

2 Theory

In this section we discuss the theoretical basis of the 2-D approximation and demonstrate that 2-D moisture tracing is exact, meaning "identical to 3-D moisture tracing", if the "well-mixed" assumption is valid. We demonstrate that well-mixed conditions are necessary for 2-D moisture tracing to be exact for two reasons. The first concerns the question from which height precipitation is drawn, and the second relates to the impact of wind shear on horizontal moisture advection.

The "well-mixed" assumption states that water molecules of different origin are perfectly mixed in the vertical dimension, i.e. that the fraction f_i of any WVT species i in total moisture is independent of height z (m):

$$f_i(z) = \frac{q_i(z)}{q(z)} \stackrel{!}{=} \hat{f}_i \;\forall\, z \tag{1}$$

where q_i (kg kg^{-1}) is the specific concentration of moisture stemming from the source region i, q (kg kg^{-1}) is the total specific moisture $q = \Sigma_i q_i$, and

$$\hat{f}_i = \frac{\hat{q}_i}{\hat{q}} \tag{2}$$

with

$$\hat{q}_i = \int_0^\infty \rho\, q_i \, \mathrm{d}z \tag{3}$$

and

$$\hat{q} = \int_0^\infty \rho\, q \, \mathrm{d}z \tag{4}$$

where ρ (kg m^{-3}) is the air density. Here and in the following we simplify the notation inside integrals by dropping the argument that indicates the dependency of the variables on z (a notation that we adopt also for the other spatio-temporal dimensions).

If the "well-mixed" assumption (Eq. 1) does not hold, the composition of precipitation P arriving at the surface depends on the height from which the moisture originates:

$$\frac{P_i}{P} = \frac{\int_0^\infty f_i\, p^* \, \mathrm{d}z}{\int_0^\infty p^* \, \mathrm{d}z} \tag{5}$$

where P_i (kg m^{-2}) is the amount of precipitation that stems from the source region i and $p^*(z)\,\mathrm{d}z$ (kg m^{-2}) is the amount of precipitation drawn from the height z. It is obvious that p^* can be interpreted as a vertical weight function. Note, however, that p^* is not simply the (vertically resolved) difference of condensation and re-evaporation, but the result of a downward propagating integrative process that involves additional assumptions regarding the gross terms of condensation and evaporation (see below). Only if the "well-mixed" assumption (Eq. 1) holds, Eq. (5) becomes $P_i/P = \hat{f}_i$, i.e. the vertical dimension does not need to be resolved to correctly determine the composition of precipitation.

We now turn to the second reason why 2-D moisture tracing requires well-mixed conditions to be exact, which concerns horizontal advection. To this end we start from the full 3-D transport (advection) equation, and derive the 2-D formulation by vertical integration. For the sake of simplicity we omit one of the two horizontal dimensions. The full transport equation for a WVT species i without sources and sinks reads

$$\frac{\partial(\rho\, q_i)}{\partial t} + \frac{\partial(\rho\, q_i\, u)}{\partial x} + \frac{\partial(\rho\, q_i\, w)}{\partial z} = 0 \tag{6}$$

where u (m s^{-1}) is the wind speed along the horizontal dimension x (m), and w (m s^{-1}) is the wind speed along the vertical dimension. In large-scale AGCMs the vertical term can only partly be handled explicitly because subgrid-scale processes ("turbulent diffusion") typically dominate the vertical transport. Turbulent (convective) processes are therefore handled by additional parameterisations.

Vertical integration of Eq. (6) gives

$$\int_0^\infty \frac{\partial(\rho\, q_i)}{\partial t}\, \mathrm{d}z + \int_0^\infty \frac{\partial(\rho\, q_i\, u)}{\partial x}\, \mathrm{d}z = 0. \tag{7}$$

The integral of the vertical term in Eq. (6) is zero because $w = 0$ for $z = 0$ and $\rho \to 0$ for $z \to \infty$. Equation (7) can be rewritten as

$$\frac{\partial \hat{q}_i}{\partial t} + \frac{\partial\left(\hat{q}_i\, \hat{u}_i\right)}{\partial x} = 0 \tag{8}$$

with

$$\hat{u}_i = \frac{\int_0^\infty \rho\, q\, f_i\, u \, \mathrm{d}z}{\int_0^\infty \rho\, q\, f_i \, \mathrm{d}z}. \tag{9}$$

Here, $\hat{u}_i$ is a tracer-density-weighted vertical average of the horizontal wind speed, and multiplication of $\hat{u}_i$ with the vertically integrated tracer mass $\hat{q}_i$ gives the vertically integrated horizontal flux of the WVT species i. $\hat{u}_i$ can thus be interpreted as an effective wind speed at which the WVT species i is horizontally advected.

If f_i varies with height, $\hat{u}_i$ is generally different for different tracer species i. If, however, the "well-mixed" assumption holds, f_i drops out of Eq. (9) and, hence, $\hat{u}_i$ becomes

the WVT-species independent effective wind speed $\hat{u}$:

$$\hat{u}_i = \hat{u} = \frac{\int_0^\infty \rho\, q\, u \, \mathrm{d}z}{\int_0^\infty \rho\, q \, \mathrm{d}z} \; \forall \, i. \tag{10}$$

This in turn leads to the horizontal advection equation of the 2-D approximation:

$$\frac{\partial \hat{q}_i}{\partial t} + \frac{\partial \left(\hat{q}_i \, \hat{u} \right)}{\partial x} = 0 \, . \tag{11}$$

As the derivation shows, this relation is exact if f_i is independent of height, i.e. if the "well-mixed" assumption holds (Eq. 1).

But not only well-mixed conditions may lead to exact 2-D tracing: Eq. (9) further reveals that $\hat{u}_i = \hat{u} \; \forall \, i$ is also obtained if the horizontal winds are not sheared vertically, meaning that in this case the 2-D-approximated horizontal advection term is exact irrespective of the validity of the "well-mixed" assumption. However, without well-mixed conditions the determination of the composition of precipitation would still require vertically resolved tracer fields (see Eq. 5).

In summary, the results of the above considerations are as follows:

- If the atmospheric moisture is perfectly well-mixed vertically, the 2-D approximation is exact. This is true even if the horizontal winds are sheared vertically.

- If the atmospheric moisture is not well-mixed but the horizontal winds are vertically uniform, the 2-D advection term is exact. However, in this case the composition of precipitation cannot be determined exactly without resolving the vertical dimension.

Of course, in reality the atmosphere is neither perfectly well-mixed vertically, nor are the horizontal winds vertically uniform. However, the above analysis reveals that the size of errors introduced by 2-D moisture tracing must depend on the degree to which atmospheric conditions deviate from these limit cases. Therefore, we investigate in the next section key characteristics of the atmosphere that largely influence the above mentioned factors, and analyse in Sect. 5 to what extent 3-dimensionally simulated atmospheric conditions deviate from well-mixed conditions.

3 Methods

3.1 ECHAM6

The numerical simulations underlying the present study are performed with ECHAM6 (Roeckner et al., 2003; Stevens et al., 2013), the atmosphere–land component of the Earth system model developed at the Max Planck Institute for Meteorology (MPI-ESM). The model is run at resolution T63/L47, which features $1.875^\circ \times 1.875^\circ$ horizontal grid spacing, a 10 min time step, and 47 vertical levels. Of the latter, 22 are below 200 hPa, and the lowest layer spans ∼8 hPa (∼60 m). Climatological sea surface temperatures (SSTs) representing present-day conditions without interannual variability are prescribed.

Tracers in ECHAM6, including atmospheric water in gaseous, liquid, and solid states, are horizontally advected with a flux-form semi-Lagrangian scheme introduced by Lin and Rood (1996). Vertical diffusion of tracers is implemented with the eddy diffusion method where the diffusivity is parameterised in terms of the turbulent kinetic energy (e.g. Garratt, 1992). Vertical redistribution of tracers is also caused by moist convection. The latter is implemented in ECHAM6 with a Tiedtke–Nordeng scheme (Tiedtke, 1989; Nordeng, 1994) where a distinction is made between shallow, mid-level, and deep convection (see also Möbis and Stevens, 2013). No horizontal diffusion is applied to tracers.

3.2 WVTs

In addition to being transported as a passive tracer in ECHAM6, atmospheric moisture is transported downward by precipitation. The vertically resolved precipitation fluxes can in principle be taken directly from the internal (prognostic) variables of the model. However, due to numerical issues related to the implementation of the flux-form advection scheme (Jöckel et al., 2001) and also due to the moist convective parameterisation, ECHAM6 is not completely conserving water mass. We therefore decided to use an alternative method to diagnose the vertically resolved precipitation fluxes, ensuring that the sum over all WVTs is permanently equal to the prognostic moisture of the model. The method is described in detail in Appendix A.

In this paper we consider the results of online 3-D moisture tracing as the "truth" to which we compare the results of the 2-D moisture tracing. However, online 3-D moisture tracing itself bears some uncertainty in the way it is implemented, even if the AGCM is assumed to be perfect. The reason is that, while the net exchange of water molecules between falling raindrops and the ambient air is part of the implementation of an AGCM, assumptions have to be made regarding the degree to which gross re-evaporation and gross condensation act to mix the precipitation with the ambient water vapour. We implemented two different 3-D moisture tracing variants, called 3-D-ref and 3-D-mod, described in Appendix A, to examine the uncertainty associated with this issue. The results, summarised in Appendix B, are however similar enough to use just one of the 3-D variants (3-D-ref, the one that is probably more realistic) as reference for the subsequent investigations.

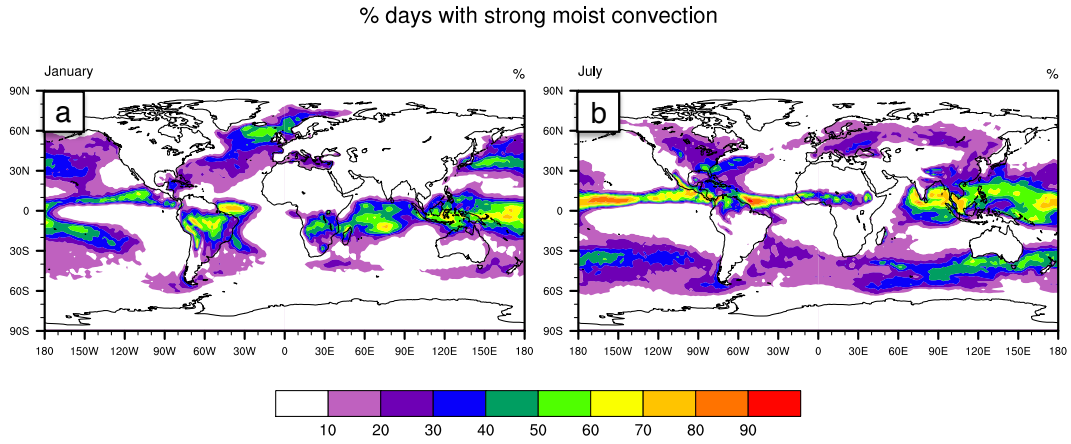

Fig. 1. Fraction of days with strong moist convection for January and July, where we consider events as strong if the generated daily amount of convective precipitation exceeds 10 % of the total column water content.

In Sect. 2 we showed analytically that the 2-D approximation is exact if the "well-mixed" assumption is valid. In this case 2-D and 3-D moisture tracing are identical. Technically, one can thus convert the full 3-D tracing to a scheme that is equivalent to 2-D moisture tracing by imposing artificially well-mixed conditions. Based on this, our 2-D moisture tracing variant is derived from the 3-D implementation by mixing completely the WVTs in each atmospheric column after every model time step (see Appendix A).

3.3 Experimental setup

To make sure that our results are not impaired by the moisture of unknown evaporative origin contained in the atmosphere at the beginning of the simulations, we added an "initial" tracer that has the same concentration as the prognostic moisture of the model at the initial time of the simulation. After the first (transient) year, the amount of initial tracer left in the troposphere was negligible. Since we used prescribed climatological SSTs, the physical model state can also be considered to be close to a quasi-equilibrium state after one year. All results that we show are averaged over the last 10 yr of 11 yr long integrations.

The moisture tracing is completely passive, meaning that the WVTs do not affect the evolution of the physical model state. This allowed us to simulate the moisture tracing with the different tracing variants described above on top of binary identical model runs by using identical initial conditions. We can thus attribute any differences between the results of the tracing variants exclusively to the differences between their implementation. Altogether we performed nine (physically identical) integrations in which we applied the three tracing variants (3-D-ref, 3-D-mod, and 2-D) to three sets of evaporative source regions (defined below).

4 Relevant characteristics of the atmosphere

Whether or not the atmosphere is well-mixed vertically depends on the interplay between vertical mixing on the one hand and the generation of vertical inhomogeneities on the other. In this section we discuss the key mechanisms that lead to vertical inhomogeneities and, hence, to inaccuracies associated with 2-D moisture tracing.

4.1 Vertical mixing

First we consider the strength of vertical mixing. The lowest $\sim$1000 m of air constituting the atmospheric boundary layer are to a first-order approximation continuously mixed by turbulent motions caused by surface friction and dry convection. In contrast, the free troposphere above experiences rather sporadic mixing through the action of deep and mid-level moist convection. While the relatively warm and hence moist boundary layer usually contains a large fraction of the atmospheric moisture, the higher wind speeds in the free troposphere above have the effect that the free troposphere considerably contributes to the horizontal moisture flux. These considerations suggest that the frequency of strong moist convective events may be a useful indicator for the degree of vertical mixing. We define moist convective events to be strong if the daily amount of convective precipitation exceeds 10 % of the total vertically integrated atmospheric water content, where the latter is averaged over the respective day (Fig. 1).

Strong moist convection occurs frequently in the tropical rain belt, which shifts its position during the course of the year, and in the extratropical storm track regions (Fig. 1). In the latter the signal is strongly seasonal: over the ocean, the frequency of strong moist convection is much higher during the respective hemisphere's winter, i.e. when the storm tracks are more pronounced. In contrast, over the northern extratropical continents strong moist convection is more

frequent in northern summer. These patterns indicate qualitatively when and where vertical inhomogeneities with respect to moisture composition can be expected to relax quickly towards well-mixed conditions.

4.2 Generation of vertical inhomogeneities

Of course it is not only the strength of vertical mixing, but also the degree to which inhomogeneities in the vertical moisture distribution are generated that determines whether the atmosphere attains an approximately well-mixed state. We now consider two factors that are responsible for the generation of vertical inhomogeneities.

First, vertical inhomogeneities with respect to moisture composition are generated by surface evaporation, which acts to enrich moisture of local origin in the lower part of the atmosphere. One may consider surface evaporation as the primary cause of vertical inhomogeneities. Second, vertical inhomogeneities can be generated by advection if the horizontal winds are sheared vertically. This mechanism may be considered as a secondary cause of vertical inhomogeneities because it generates vertical inhomogeneities out of horizontal inhomogeneities. If the horizontal winds are sheared vertically, the composition of different layers in the atmosphere can be very different, in particular if vertical mixing is weak.

An idea to what extent the winds are sheared vertically can be obtained by comparing monthly means of the near-surface (925 hPa) winds and the mid-tropospheric (650 hPa) winds (Fig. 2a–d). For a more quantitative assessment, one also has to take into account that the specific humidity of the air decreases steeply with height due to the temperature gradient, meaning that the same windspeed is associated with stronger moisture transport in lower levels than in higher levels.

It stands to reason that directional shear of the horizontal wind is more effective in generating vertical inhomogeneities than speed shear of the horizontal wind; in case of vertically uniform wind directions but varying wind speeds, a relatively low degree of vertical mixing may suffice to maintain close to well-mixed conditions. We therefore introduce a measure Γ that quantifies the degree to which shear generates vertical inhomogeneities as follows:

$$\Gamma := \frac{\left\| \int_0^\infty \rho q \begin{pmatrix} u \\ v \end{pmatrix} \mathrm{d}z \right\|}{\int_0^\infty \left\| \rho q \begin{pmatrix} u \\ v \end{pmatrix} \right\| \mathrm{d}z} \tag{12}$$

where z is geometrical height, ρ is air density, q is specific humidity, u and v are the zonal and the meridional component of the horizontal wind, and $\|\cdot\|$ is the Euclidean norm. While the numerator is proportional to the absolute value of the vertically integrated horizontal moisture flux (Fig. 2e–f), the denominator is proportional to what this flux would be if the winds at all heights pointed in the same direction (with the same orientation). Obviously, $\Gamma \in [0, 1]$, with low values indicating strong directional shear of the horizontal moisture flux and high values indicating weak directional shear of the horizontal moisture flux. In the following we refer to Γ simply as directional shear.

Γ (computed for 6-hourly data) reveals that strong directional shear is mostly confined to the tropics (Fig. 3). This is due to the fact that the weak Coriolis force near the equator allows the development of thermally direct circulations, while in the extratropics the Coriolis force acts to establish flow in approximate geostrophic balance, leading to vertically more uniform wind directions. Another striking feature is that strong directional shear often occurs at continental coasts, for example at the South American and African western coasts both in January and in July, and in a band ranging from the Gulf of Oman over India and Indochina to the Philippine Sea in January. This feature supports the supposition that directional shear is mainly caused by thermally direct circulations, because the latter are typically strongest in the vicinity of continental coasts.

Considered together, the frequency of strong moist convection (Fig. 1) and the magnitude of directional shear (Fig. 3) provide a qualitative idea of when and where the atmosphere may attain close to vertically well-mixed conditions, meaning that 2-D moisture tracing may be an appropriate approximation. A more quantitative assessment of whether the atmosphere is well-mixed, and how large the errors associated with the 2-D approximation are, is the subject of the following two sections.

5 On the validity of the "well-mixed" assumption

In Sect. 2 we showed analytically that the 2-D approximation is exact if the fractions of all WVT species are perfectly well-mixed vertically. Therefore, before comparing results of 2-D and 3-D moisture tracing (Sect. 6), we investigate in this section to what extent the WVT species from different evaporative source regions are actually well-mixed vertically. To this end we analyse results obtained for two sets of source regions with 3-D moisture tracing (variant 3-D-ref, see Appendix A).

The first set of source regions is defined by the land–sea mask of the model, meaning that only oceanic and continental moisture are distinguished. In the second set we distinguish four evaporative source regions, of which three are defined by 1000 km × 1000 km-rectangles located on different continents (Table 1, marked by black boxes in Figs. 5 and 7) while the fourth comprises the remainder of the Earth's surface.

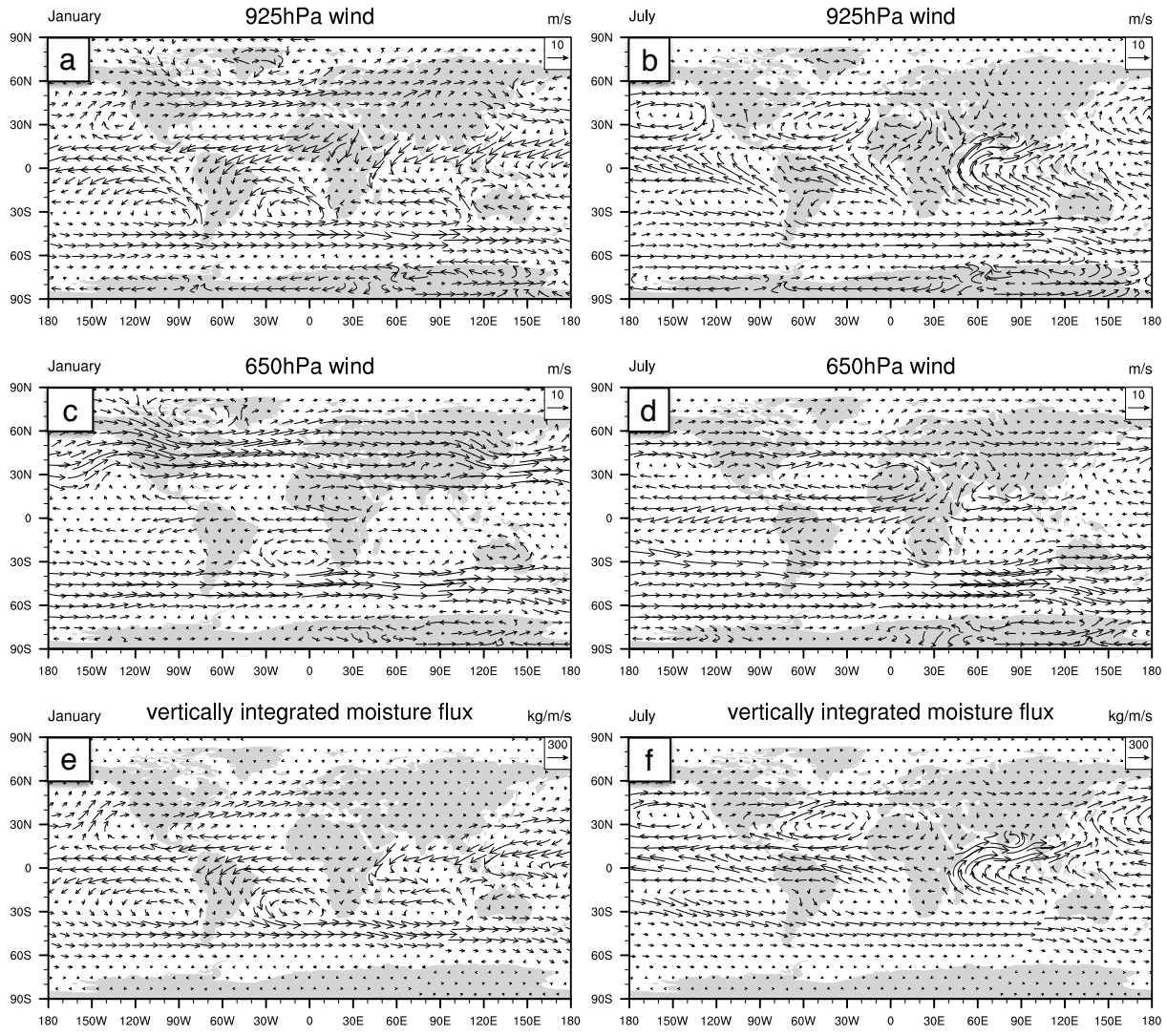

Fig. 2. Horizontal winds at 925 hPa ($m\,s^{-1}$) and 650 hPa ($m\,s^{-1}$), and vertically integrated moisture flux ($kg\,m^{-1}\,s^{-1}$), for January and July.

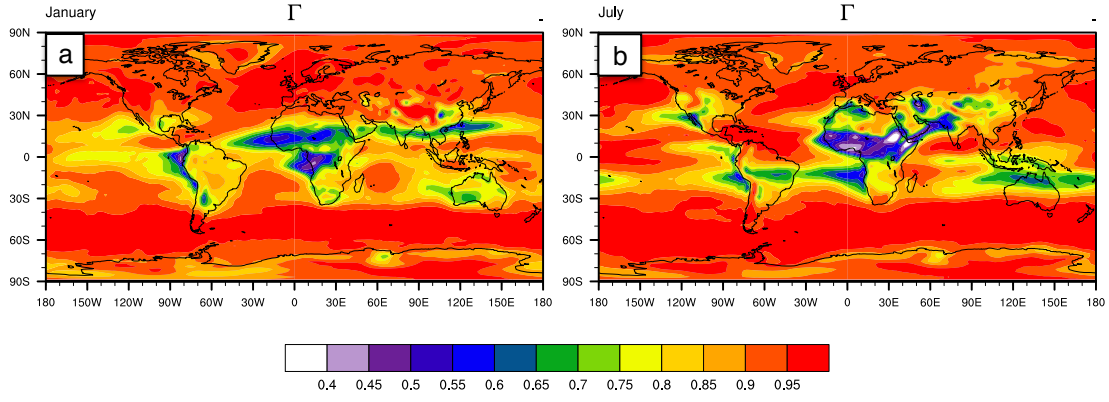

Fig. 3. Directional shear as measured by Γ (Eq. 12) for January and July. To compute the monthly averages shown in this figure, numerator and denominator in the definition of Γ (see Eq. (12)) are averaged separately over time.

Table 1. Locations of the 1000 km-scale rectangular source regions.

Name	abbrev.	meridional range (° N)	zonal range (° E)
Eastern Europe	EEU	50.4–59.7	30.9–47.8
Amazonia	AMA	−9.3–0.0	295.3–304.7
Western Africa	WAF	7.5–16.8	0.0–9.3

To quantify to what extent a WVT species i is well-mixed vertically we define the measure Ψ_i as follows:

$$\Psi_i := 2\,\frac{\int_{z^*}^{\infty} \rho\, q_i \,\mathrm{d}z}{\int_0^{\infty} \rho\, q_i \,\mathrm{d}z} - 1 \tag{13}$$

where z^* is determined by

$$\frac{\int_{z^*}^{\infty} \rho\, q \,\mathrm{d}z}{\int_0^{\infty} \rho\, q \,\mathrm{d}z} = 0.5, \tag{14}$$

which means that half of the total atmospheric moisture resides above z^* and the other half resides below z^*. Obviously, $\Psi_i \in [-1, 1]$, with $\Psi_i = 0$ indicating well-mixed conditions and negative (positive) values indicating higher concentrations in the lower (upper) half of the atmospheric moisture column. Computing Ψ for the moisture of continental origin (Fig. 4) and for the moisture stemming from the three rectangular source regions (Fig. 5) reveals that well-mixed conditions are overall rather scarce.

In Sect. 4 we argued qualitatively that whether or not the atmosphere is close to well-mixed vertically results from the interplay between the generation of vertical inhomogeneities on the one hand and the strength of vertical mixing on the other. While vertical inhomogeneities are generated by surface evaporation and by directional shear (Fig. 3), vertical mixing that involves not just the boundary layer but also the free troposphere occurs to a large part through the action of moist convection (Fig. 1). The fact that well-mixed conditions are relatively rare (Figs. 4 and 5) means that vertical mixing is mostly not strong enough to nullify the generation of inhomogeneities by surface evaporation and directional shear.

The influence of surface evaporation on Ψ is straightforward: while within the respective source region surface evaporation acts to enrich moisture originating from the region in the lower levels of the atmosphere (decreasing Ψ) directly, outside the respective source region surface evaporation acts to enrich moisture originating from the region in the upper levels indirectly by enriching moisture of different origin in the lower levels (increasing Ψ_i). This effect is clearly visible in the patterns of Ψ (Figs. 4 and 5): Ψ_{cont} is mostly negative over land and positive over the ocean, and Ψ_{EEU}, Ψ_{AMA}, and Ψ_{WAF} are mostly negative within the respective regions and positive outside.

Strongly negative values of Ψ inside the source regions only occur where strong moist convection is rare (Fig. 1). Otherwise, a substantial enrichment of local moisture in the lower levels is prevented by vertical mixing. For Ψ_{cont} this is the case, for example, in large parts of South America in January and in large parts of Eurasia in July. In the case of the smaller-scale regions, close to well-mixed conditions inside the region itself occur only in AMA in January due to the vigorous daily mixing by deep convection. At the other extreme are the conditions in EEU in January: here, almost all moisture stemming from the region is concentrated in the lower half of the atmospheric moisture – not only inside the region itself but in large parts of the Northern Hemisphere. This reflects the stable atmospheric stratification that prevails during the northern-hemispheric winter over the northern land and sea-ice areas, effectively suppressing strong moist convection (Fig. 1).

It is generally an interesting question at which distance from the source regions well-mixed conditions are attained by vertical mixing. Apart from the just mentioned case of EEU in January, negative values of Ψ directly associated with the regions' surface evaporation are mostly constrained to the close proximity of the respective source regions (Figs. 4 and 5). This means that vertical inhomogeneities generated inside the regions typically do not persist for more than a couple of hundred kilometres until vertical mixing has largely nullified the inhomogeneities. Besides the special case of EEU in January, it seems that also in most of the other cases negative values of Ψ generated inside the source regions are preserved for considerably more than a few hundred kilometres at least in one direction, for example in July to the south of EEU, to the north-west of AMA, and to the east of WAF.

Inspection of the vertical structure of the winds (Fig. 2a–d and Fig. 3), however, reveals that it is rather directional shear that is responsible for these negative-Ψ-tails, meaning that they are not simply due to the preservation of the low-level enrichment generated inside the source regions. For example, the tail to the north-west of AMA and the tail to the east of WAF, both in July, are due to a situation where low-level winds advect air masses directly from the respective source region while mid-tropospheric winds blow from a different direction. An analogous situation leads to negative values of Ψ_{EEU} to the south of EEU in July where the westerlies have a significant southward component that is absent in the mid-troposphere. However, in the latter case the "tail" with negative values of Ψ_{EEU} covers a much larger area because the subsiding branch of the Hadley cell south of $\sim 35°$ N is associated with virtual absence of strong moist convection (Fig. 1), meaning that vertical inhomogeneities are preserved once air masses have entered the subtropics from the north.

Beyond the primary regions of low-level enrichment (negative Ψ) in the vicinity of the respective source regions, Ψ not only attains values around zero, corresponding to well-mixed conditions, but is mostly positive (Fig. 5). As

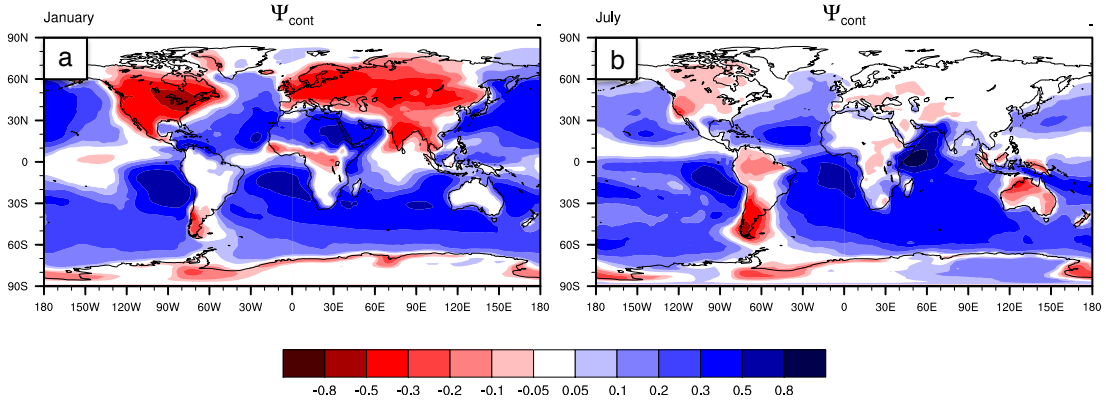

Fig. 4. The degree to which moisture of continental origin is over-represented in the upper half (positive values) or the lower half (negative values) of the atmospheric moisture column (Ψ_{cont}, Eq. 13), for January and July, as simulated with 3-D-ref.

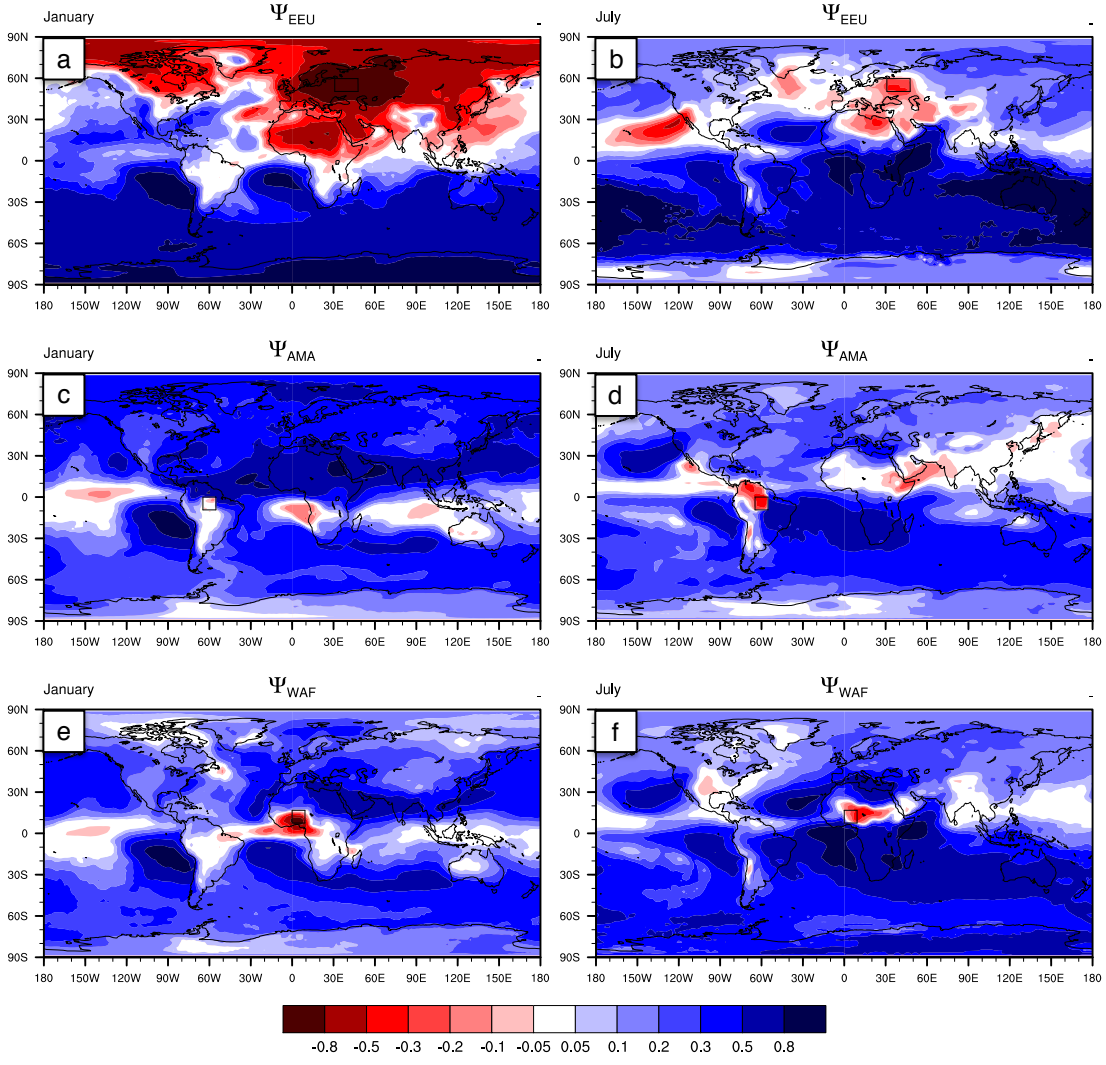

Fig. 5. The degree to which moisture originating from the regions EEU (Ψ_{EEU}), AMA (Ψ_{AMA}), and WAF (Ψ_{WAF}) is over-represented in the upper half (positive values) or the lower half (negative values) of the atmospheric moisture column (Eq. 13), for January and July, as simulated with 3-D-ref.

mentioned above, this is primarily due to the action of surface evaporation. However, apart from the narrow transition zones, i.e. where Ψ switches its sign, close to well-mixed conditions also occur in some more distant locations. Most striking is a band of close to well-mixed conditions for all considered source regions (Figs. 4 and 5) near the equator, which is obviously due to strong mixing caused by frequently occurring deep convection within the Intertropical Convergence Zone (ITCZ) (Fig. 1).

Well-mixed conditions, and even low-level enrichment, at locations far away from the respective source regions can also be generated by a suitable vertical structure of the winds. Here, suitable means that, compared to the high-level winds, the low-level winds advect air from regions containing higher fractions of moisture stemming from the considered source region. This is, for example, the reason for the negative values of Ψ_{AMA} and Ψ_{WAF} above the tropical Eastern Pacific in January, and also for the negative values of Ψ_{EEU} between Hawaii and California in July (Fig. 5). In the latter case, near-surface winds advect extratropical air masses from the north while mid-tropospheric easterlies advect tropical air masses from the east (Fig. 2b, d). Because the overall prevailing zonal winds act to mix air masses faster zonally than meridionally, air masses located within the same zonal band as the source region under consideration contain tendentially more moisture stemming from the source region than air masses in other zonal bands. This explains not only why Ψ_{EEU} is strongly negative between Hawaii and California in July, but also why Ψ_{AMA} and Ψ_{WAF} are strongly positive at the same time and place. Moreover, the fact that mixing occurs faster in zonal than in meridional direction also explains why, apart from the direct vicinity of the tropical source regions, the patterns of Ψ_{AMA} and Ψ_{WAF} are generally similar.

6 2-D versus 3-D moisture tracing

In the following we compare results obtained with 2-D moisture tracing with results obtained with 3-D moisture tracing (variant 3-D-ref, see Appendix A), focussing on the simulated composition of precipitation. First we discuss results from the same two sets of evaporative source regions considered in the previous section. Thereafter we investigate a third set of source regions that serves to determine the evaporative sources of precipitation in the western Sahel region. It has already been hypothesised that the 2-D approximation may lead to large errors in this region (Goessling and Reick, 2011; Dirmeyer, 2011).

6.1 Continental and oceanic source region

We begin with the tracing experiments in which a distinction is made between moisture of continental and oceanic origin. We analyse the fractions of precipitation stemming from continental evaporation (compare Eq. (5)). These are the so called "continental precipitation recycling ratios". Following Goessling and Reick (2011), these will be called simply "continental recycling ratios" and are denoted by R_{c}.

2-D and 3-D moisture tracing give comparable continental-scale patterns of the continental recycling ratio (Fig. 6a–d). In agreement with earlier studies (Numaguti, 1999; Bosilovich et al., 2002; Yoshimura et al., 2004; van der Ent et al., 2010; Goessling and Reick, 2011), we find that R_{c} increases from continental upwind coasts to downwind coasts (see also Fig. 2e–f) with weak seasonality in the tropics and strong seasonality in the extratropics. The latter is mainly due to the seasonality of evaporation (not shown). While the highest values of R_{c} occur in Eastern Eurasia in July with more than 80 %, peak values in the continental tropics are around 60 % throughout the year.

While the continental-scale patterns are overall similar, there are systematic differences in R_{c} as simulated with 2-D and 3-D tracing (Fig. 6e–f). Most strikingly, 2-D tracing gives mostly lower values on the continents and higher values over the ocean. This land–ocean contrast is clearer in the northern extratropics than in the tropics. The amplitude of this difference pattern amounts to about ± 10 % in the northern extratropics in July, with the Arctic and the North Atlantic featuring higher values, and North America and western Eurasia featuring lower values when 2-D tracing is applied. The maxima of the differences between 2-D and 3-D tracing tend to be even larger in the tropics. Here, differences in R_{c} in some places amount to more than ± 20 %.

The land–ocean contrast in the difference pattern can largely be explained with fast-recycling, a term coined by Lettau et al. (1979). Fast-recycling means that moisture of local origin is over-represented in precipitation. Fast-recycling occurs if (i) the locally evaporated moisture is not (yet) effectively mixed vertically and thus over-represented close to the surface, and (ii) the precipitating water stems preferentially from this near-surface portion of the atmosphere.

That the first of these conditions is fulfilled (when 3-D tracing is applied) can be seen from Ψ_{cont} (Fig. 4): On the continents the fraction of continental moisture in total moisture is larger near the surface than in higher levels. The same holds for oceanic moisture over the ocean. The second condition (precipitation stems from near-surface air) is by construction fulfilled for the particular 3-D-ref tracing variant used here (compare Eq. A8), but simulations show similar results for the alternative extreme variant 3-D-mod (see Appendix B for an assessment on how sensitive the results are on the tracing variant). This implies that 3-D tracing features fast-recycling. The complete neglect of fast-recycling in the case of 2-D tracing is the reason for the land–ocean contrast seen in the difference pattern of R_{c} (Fig. 6e–f).

While fast-recycling is apparently the main reason for errors associated with the 2-D approximation in the extratropics, another factor comes into play in the tropics. Here, the spatial patterns of R_{c} derived with 2-D and 3-D tracing exhibit a characteristic structural difference: the

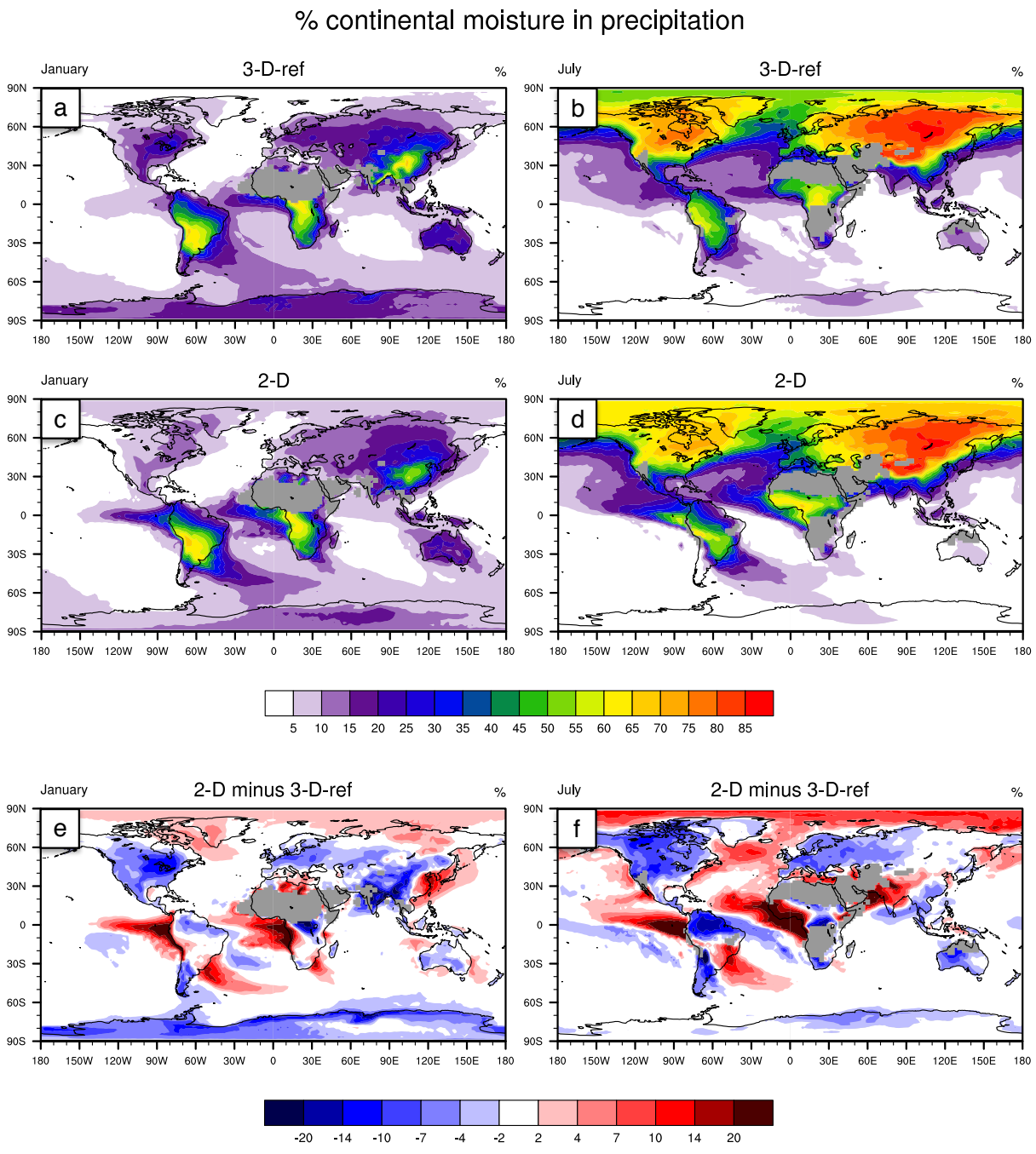

Fig. 6. Continental recycling ratios (R_C, % continental moisture in precipitation) as simulated with 3-D-ref and 2-D, and the difference between two, for January and July. Grey areas are masked because less than five out of the ten years used for computing the averages have non-zero precipitation in the considered month, leading to statistically non-robust estimates.

continental recycling ratios derived with 2-D tracing tend to have steeper gradients, most strikingly to the west of both Africa and South America in the vicinity of the equator. Also, while in the extratropics errors introduced by the 2-D approximation are rather shape preserving, the errors in the tropics are associated with changes in the shape of the patterns of R_C.

The reason for these structural differences (the steeper gradients and the modified pattern shapes obtained with 2-D tracing) is that in the tropics directional shear (Fig. 3) causes basically horizontal dispersion of atmospheric moisture components, resulting in smoothed horizontal gradients. This effect is missing in the vertically integrating 2-D approach. It is hence in these tropical regions where the largest differences,

not only in magnitude but also in shape, between continental recycling ratios obtained with 2-D and 3-D moisture tracing occur.

6.2 1000 km-scale source regions

The already described difference between the tropics and the extratropics is also evident in the results for the three smaller evaporative source regions (Fig. 7). Within EEU the 2-D approximation substantially underestimates the fraction of local moisture in precipitation, and outside EEU the fraction of moisture from EEU in precipitation is overestimated. The main explanation for this is, again, the neglect of fast-recycling. For the tropical regions AMA and WAF there is apparently also an element of this, causing mostly an underestimation of recycling within the source regions and an overestimation outside. However, the shape of the resulting patterns is considerably altered by the 2-D approximation only in the tropics. This is most obvious in July: while 3-D tracing reveals that moisture evaporated from WAF is preferentially advected north-eastward (Fig. 7b), the results of the 2-D approximation suggest that the moisture is mainly advected westward (Fig. 7d). For moisture evaporated from AMA in July, 3-D tracing gives highest fractions in precipitation along the western boundary of the source region, whereas the 2-D approximation gives peak values in the south-western corner. An even more salient difference in this case is that the 2-D approximation diagnoses that substantial amounts of moisture stemming from AMA precipitate over the tropical Eastern Pacific – a feature that the full tracing reveals as an artefact.

These errors in the tropics are obviously due to the layered structure of the atmosphere. In AMA in July, the monsoonal layer below ~ 750 hPa carries air masses north-eastward while the African easterly jet above ~ 750 hPa blows westward (Fig. 2b, d). Due to the high wind speeds, the horizontal moisture flux associated with the African easterly jet outweighs the flux associated with the moister but slower moving monsoonal layer, explaining why the 2-D variant diagnoses a westward advection of moisture (Fig. 2f). This leads to erroneous results because most of the moisture stemming from WAF is concentrated in the north-westward flowing monsoonal layer (Fig. 5f). An analogous explanation can be given for the differences seen in AMA in July described above, where the prevailing easterlies have a northward component near the surface but a southward component in the mid-troposphere (Fig. 2b, d), combined with considerably non-zero values of Ψ_{AMA} (Fig. 5d).

The meteorological conditions in these regions are different in January. At this time of the year WAF is subject to subtropical large-scale subsidence, the ITCZ being located further to the south. Because of the associated absence of precipitation, this region is not very interesting in the context of our study at that time of the year. By contrast, AMA, located south of the equator, receives considerably more precipitation in January than in July. The higher frequency of strong moist convection in January (Fig. 1) is associated with stronger vertical mixing. This, in combination with a relatively low degree of directional shear (Fig. 3), acts to prevent significant enrichment of local moisture near the surface (Fig. 5c). Consequently, in AMA in January the 2-D approximation gives reasonable results, the only deficit seeming to be the neglect of a moderate degree of fast-recycling (Fig. 7a, c, e).

Comparing the results for the 1000 km-scale source regions with those for the continental recycling ratio reveals that the accuracy of the 2-D approximation is to a certain degree scale dependent. In relative terms, the simulated patterns are overall less biased if large-scale source regions are considered (Fig. 6a–d) than if smaller-scale source regions are considered (Fig. 7a–d). This scale dependence arises mainly from the fact that fast-recycling is more relevant at smaller scales: the larger the scale, the more time there is for vertical mixing to reduce vertical inhomogeneities. This is confirmed by the finding that the moisture from the 1000 km-scale source regions tends to be stronger over-represented close to the surface within the respective regions (Fig. 5) than the continental moisture is on average close to the continental surface (Fig. 4).

6.3 Source regions for western Sahelian precipitation

As discussed above, the transport of moisture evaporated from WAF in July can be determined only poorly using the 2-D approximation. The reason for this is that, given the strong generation of vertical inhomogeneities by surface evaporation and by directional shear, the counteracting degree of vertical mixing does not suffice to establish well-mixed conditions. This already indicates that, likewise, the evaporative source regions for precipitation in the nearby located western Sahel can probably not be diagnosed adequately using the 2-D approximation.

Keys et al. (2012) diagnosed the evaporative sources for precipitation in the western Sahel (and other regions), applying 2-D moisture tracing to ERA-Interim reanalysis data. In the following we investigate how much error in this specific case must be expected to arise from the use of the 2-D approximation. To this end we investigate moisture tracing also for a third set of evaporative source regions comprising Africa as a whole (AFR), those regions located to the south-west of Africa (SW), those regions located to the south-east of Africa (SE), and the remainder, i.e. those regions located to the north of Africa (N) (Fig. 8). We analyse the contribution of moisture from these source regions to the precipitation in the western Sahel, namely the rectangular region ranging from 8.4° W to 17.8° E and from 11.2° N to 16.8° N (see the black rectangles in Figs. 8 and 10), which is approximately the same region as the one investigated by Keys et al. (2012).

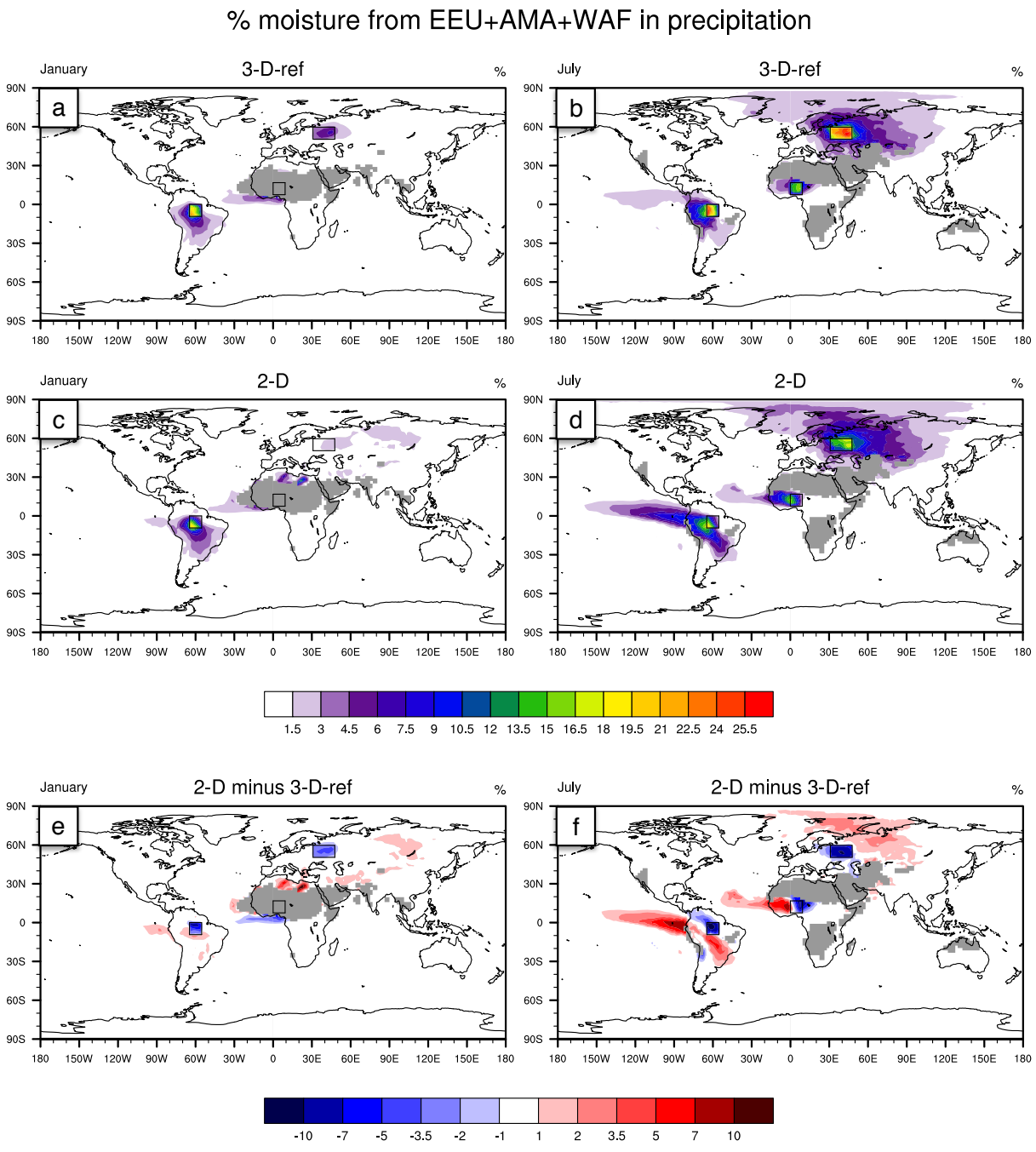

Fig. 7. The fraction of precipitation that originates from the rectangular source regions EEU, AMA, and WAF (black boxes) as simulated with 3-D-ref and 2-D, and the difference between the two, for January and July. Grey areas are masked because less than five out of the ten years used for computing the averages have non-zero precipitation in the considered month, leading to statistically non-robust estimates. Because the regions receiving significant amounts of precipitation from the three source regions are well separated, we took the liberty to show all results summed together in a single plot instead of presenting three individual plots.

The contributions to western Sahelian precipitation from AFR and SE are reasonably well reproduced by the 2-D approximation, but the contributions from N and SW are not (Table 2, Figs. 9 and 10); while 3-D tracing reveals that approximately equal amounts stem from N and SW, 2-D tracing almost completely misses the contribution from SW, compensated by an increased contribution from N. The reason for this deficit is, as already discussed for the moisture stemming from WAF, the layered structure of the atmosphere: the low-level monsoonal layer advects air masses from the south-west

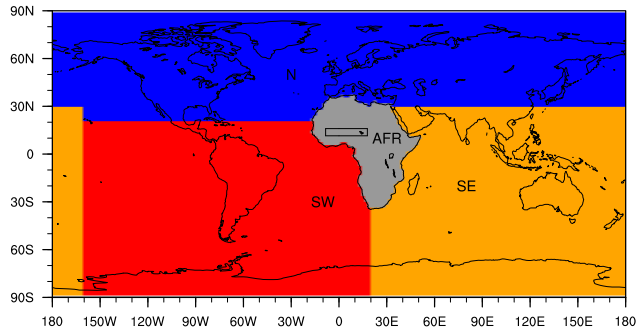

Fig. 8. The four evaporative source regions N (north), SW (south-west), SE (south-east), and AFR (Africa) that we use to determine the sources for precipitation in the western Sahel region (black rectangle).

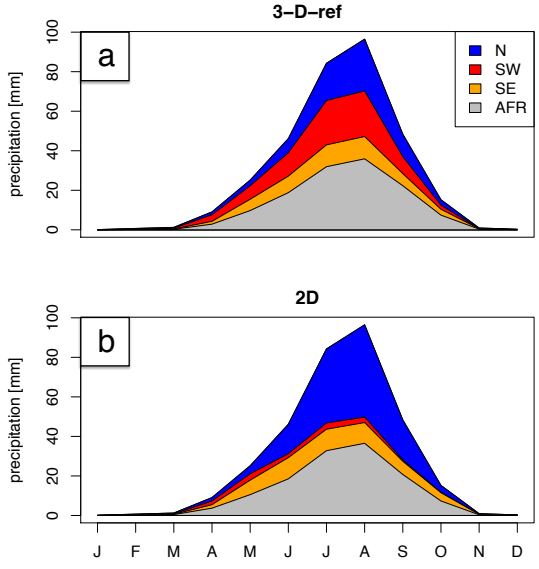

Fig. 9. Monthly absolute contribution to precipitation (mm) in the western Sahel from the four evaporative source regions (compare Fig. 8) as simulated with 3-D-ref and 2-D.

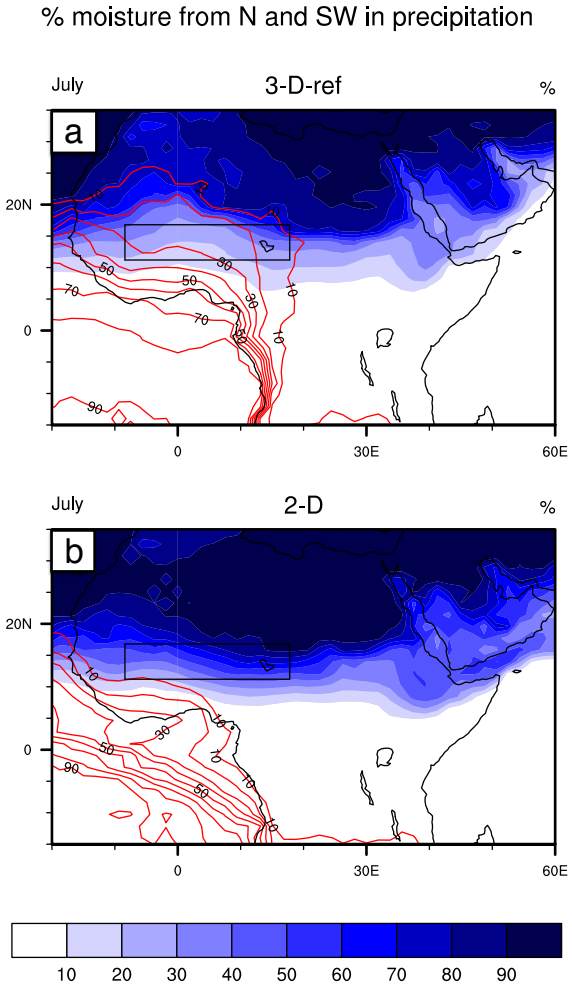

Fig. 10. Relative contribution to precipitation (%) in the western Sahel (black rectangle) in July from the regions N (blue shading) and SW (red lines) (compare Fig. 8) as simulated with 3-D-ref and 2-D.

Table 2. Contribution to annual precipitation in the western Sahel from the four evaporative source regions N, SW, SE, and AFR (compare Fig. 8) as simulated with 3-D-ref and 2-D.

Source region	3-D-ref	2-D
N	22 %	40 %
SW	24 %	4 %
SE	14 %	16 %
AFR	40 %	40 %

while the African easterly jet above advects air masses from the north-east (Fig. 2b, d, f), whereby vertical mixing is not strong enough to maintain well-mixed conditions. These results indicate that the precipitationshed of the western Sahel as determined by Keys et al. (2012) (see Fig. 3 therein) is biased towards the north-east.

This western Sahelian case provides an example where our AGCM simulations give a rather large difference between 2-D and 3-D moisture tracing. When interpreting these results, one must be aware that although our AGCM simulations reveal a quite realistic picture of the complex atmospheric structure for the tropics, quantitatively our numbers may not be fully realistic, since subtle differences in the exact geographical location of the monsoonal systems may be quite influential with respect to moisture transport. Using the data and the 2-D tracing method of Keys et al. (2012), van der Ent (2012) recalculated the moisture contributions to the western Sahel for two of the source regions used in our study. According to his calculations moisture from N contributes 26 %, and SW 10 %. This differs considerably from our 2-D results (compare Table 2). Since the study by Keys et al. (2012) is based on reanalysis data, this indicates that

our AGCM ECHAM6 underestimates the transport of moisture from the tropical Atlantic to the African continent in the monsoonal layer, and/or overestimates the advection of moisture from the north. Accordingly, our values from the 3-D-ref tracing (see Table 2) are presumably too large for N and too small for SW, meaning that the bias introduced by 2-D tracing is presumably not much affected by such a model bias.

7 Summary and conclusions

In this study we have investigated the errors that are introduced by the application of 2-D moisture tracing as opposed to the "exact" method of 3-D moisture tracing. To this end we analysed the theoretical basis of the 2-D approximation, the "well-mixed" assumption, and implemented both 3-D and 2-D moisture tracing into an AGCM, which allowed for us to make a direct quantitative comparison.

We showed analytically that 2-D moisture tracing is exact if the "well-mixed" assumption holds; in this case neither horizontal advection nor the precipitation process are associated with errors due to the 2-D approximation. Accordingly, the accuracy of the 2-D approximation is highest where meteorological conditions are favourable of well-mixed conditions, and lowest where strong vertical inhomogeneities are present. We demonstrated that key atmospheric characteristics in this context are (i) the presence of directional shear, which generates vertical inhomogeneities, and (ii) the frequency of strong moist convection, which acts to mix the atmosphere vertically. Overall, well-mixed conditions are seldom met and, hence, the 2-D approximation is mostly associated with noticeable errors.

One can discern two kinds of errors introduced by the 2-D approximation, namely (i) the omission of fast-recycling, which leads to an underestimation of local moisture in precipitation but does not greatly affect the spatial structure of the resulting patterns, and (ii) the omission of layered horizontal advection, which can have a strong impact on the spatial structure of the resulting patterns and, hence, appears to be the more serious deficit of 2-D moisture tracing.

While the presence of fast-recycling is geographically not much constrained, strongly layered advection is a distinctive feature of the tropics with its thermally direct circulations; the latter are suppressed in the extratropics where the Coriolis force gives rise to a certain vertical rigidity of the atmosphere. There are, of course, also in the tropics situations where the winds are only moderately sheared vertically and, if in combination with frequent vertical mixing, the errors resulting from the 2-D approximation are moderate. This is, for example, the case for the Amazon region in January. The rule, however, is that the 2-D approximation is less appropriate in the tropics, in particular where strong directional shear combines with a low frequency of moist convective mixing.

An example for such a region is tropical Western Africa (including the western Sahel), where in particular during the monsoon season (northern summer) the vertical structure of the atmosphere is strongly layered and moist convective mixing does by far not suffice to maintain well-mixed conditions. Here, 2-D moisture tracing strongly underestimates the amount of moisture originating from the tropical Atlantic that, in reality, is transported in the low-level monsoonal layer far into the African continent. At the same time, 2-D moisture tracing overestimates the contribution to western Sahelian precipitation originating from beyond the Sahara.

One can ask what our results imply for other offline moisture tracing methods that make use of the "well-mixed" assumption. We argue that our findings can be applied directly to other studies making thorough use of the "well-mixed" assumption in their moisture tracing method (as for example in Dominguez et al., 2006), because these methods are equivalent to 2-D tracing regarding the vertical dimension. The implications are less straightforward for methods that invoke the "well-mixed" assumption only partly, as is the case with the quasi-isentropic back-trajectory method (Dirmeyer and Brubaker, 1999). We can only speculate that this method should be overall less error-prone than 2-D tracing because the vertical shear of the winds is accounted for. On the other hand, the method does not account for fast-recycling, just like 2-D tracing. Direct comparisons would be needed to better quantify the deficits of such methods.

To conclude, we think that due to its simplicity and straightforward applicability to different kinds of data, 2-D moisture tracing can still serve as a useful first-order approximation, depending on the application. If applied, one should, however, be aware of the deficits of the method as discussed in this paper.

Appendix A

WVT implementation

A1 General implementation

In addition to being transported as a passive tracer by the wind fields of ECHAM6, our WVTs are transported downward by precipitation. Instead of making use of the internally computed vertically resolved precipitation flux of the model, the latter is diagnosed every time step as difference between the internal (prognostic) moisture q_{prog} of the model and the not yet precipitation-corrected sum over all WVT species:

$$q_{\mathrm{wvt}}(z) = \sum_{i=1}^{N} q_i(z) \tag{A1}$$

where N is the number of WVTs and q_i is the specific concentration ($\mathrm{kg\,kg^{-1}}$) of tracer i. For the method to be valid, all sources of atmospheric moisture as well as the moisture contained initially in the atmosphere must be covered by one of the WVT species.

To avert obscurities, it seems advisable to give a comment on the terms "gross" and "net" that we use in the following. Gross re-evaporation and gross condensation account for all water molecules that cross the interface between the liquid (or solid) phase and the gaseous phase (i.e. the air). The difference between these two gross terms either results in a net re-evaporation or a net condensation, depending on which of the gross terms dominates.

The procedure described in the following is applied at the end of every model time step and adjusts the sum over all WVTs q_{wvt} to the prognostic moisture q_{prog} $(=q)$ of the model. Having thus started the computations at the beginning of a time step with identical values for the internal moisture of ECHAM and for the sum over our new WVTs, towards the end of a model time-step, without provision for vertical transport by precipitation, q_{wvt} is larger than q_{prog} if the local balance of gross condensation minus gross re-evaporation ($C-R$, $((\mathrm{kg\,kg^{-1}})\,\mathrm{s^{-1}})$) is positive. This is the case if net moisture is removed from the air at cost of an increasing downward precipitation flux. On the other hand, q_{wvt} is smaller than q_{prog} if $C-R$ is negative. This is the case if moisture is added to the air by net re-evaporation of precipitation. Accordingly,

$$(C-R)(z) = \frac{q_{\mathrm{wvt}}(z) - q_{\mathrm{prog}}(z)}{\Delta t} \tag{A2}$$

where Δt (s) is the time step length. One obtains the vertically resolved precipitation flux $P(z)$ $(\mathrm{kg\,(m^2\,s)^{-1}})$ for the considered time step at any height by integrating $C-R$ from the respective height to the top of the atmosphere:

$$P(z) = \int_z^\infty (C-R)(z')\,\rho(z')\,\mathrm{d}z'. \tag{A3}$$

To check for consistency, we compared the amount of precipitation arriving at the surface as diagnosed with Eqs. (A2) and (A3) with the internally computed precipitation (plus dew) of the model. We found small discrepancies between the two for single time steps that can be attributed to violations of mass conservation within the AGCM. However, the differences become negligible when averaged over a day or more (not shown), revealing that the differences are not systematic.

Analogously to Eqs. (A2) and (A3), it holds for single WVT species that the change due to precipitation within the considered time step is

$$\frac{\Delta q_i(z)}{\Delta t} = (C_i - R_i)(z) \tag{A4}$$

and that

$$P_i(z) = \int_z^\infty (C_i - R_i)(z')\,\rho(z')\,\mathrm{d}z'. \tag{A5}$$

However, while $(C-R)$ is known (Eq. A2), $(C_i - R_i)$ is unknown. For the gross terms C_i and R_i we know that

$$C_i(z) = \frac{q_i(z)}{q_{\mathrm{wvt}}(z)}\,C(z) \tag{A6}$$

and

$$R_i(z) = \frac{P_i(z)}{P(z)}\,R(z). \tag{A7}$$

If C and R are known individually, Eqs. (A5)–(A7) constitute a closed system of equations and can be solved proceeding from the top of the atmosphere downward, allowing for deriving the change of each individual tracer species (Eq. A4). Adding these changes to the tracer concentrations q_i gives the precipitation corrected values $q_i^{\mathrm{corr}} = q_i + \Delta q_i$, so that by Eqs. (A1) and (A2), $q_{\mathrm{wvt}}^{\mathrm{corr}} = q_{\mathrm{prog}}$. Setting $q_i := q_i^{\mathrm{corr}}$ at the end of the procedure hence ensures that q_{wvt} and q_{prog} start identically into the next time step, which is necessary for the validity of our method.

However, C and R are not known individually, but only $C-R$ (Eq. A2), leaving Eqs. (A5)–(A7) underdetermined. Notably, this problem is not specific to our approach in which $C-R$ is diagnosed from the differences between q_{wvt} and q_{prog} (Eq. A2). AGCMs themselves operate only with the net term $C-R$ because the gross terms are not relevant for the physical system, i.e. the total water mass and energy balance. Hence, to trace the moisture of different origins, additional assumptions have to be made regarding the gross terms C and R in order to close the above system of equations.

A2 3-D variants

Since many complex processes are involved, determining realistic gross terms is a delicate task that is clearly beyond the scope of this paper. Instead, we implemented two different variants of the tracing with simple assumptions regarding the gross terms. The two variants reflect the two extremes regarding the question of how large the gross terms C and R are.

In the first case (variant 3-D-ref, "reference"), we assume that C and R are very large, meaning that the precipitation mixes rapidly (in case of the discrete layers of the AGCM instantaneously) with the ambient water vapour. The instantaneous equilibration leads to

$$\text{variant 3-D-ref:} \qquad \frac{P_i(z)}{P(z)} = \frac{q_i(z)}{q_{\mathrm{wvt}}(z),} \tag{A8}$$

which closes the system of equations defined by Eqs. (A5)–(A7). For a discrete model layer this case means that all precipitation entering at the top of the layer mixes with the water vapour in the layer, and that the composition of the precipitation leaving the layer at its bottom equals the composition of the resulting mixture. It is this variant that we consider in the main part of the paper.

In the second case (variant 3-D-mod, "modified", not considered in the main part of the paper), we assume that only the net exchange between the precipitation and the ambient air takes place as

$$\text{variant 3-D-mod:} \quad C(z) = \max((C - R)(z), 0), \tag{A9}$$

which implies that $R(z) = \max(-(C - R)(z), 0)$. This is an alternative to Eq. (A8) to close the system of equations defined by Eqs. (A5)–(A7). For a discrete model layer this case means the following: if net condensation occurs, the composition of the water vapour in the layer remains unchanged while only the composition of the precipitation is modified by the condensing water molecules. If, however, net re-evaporation occurs, the composition of the precipitation remains unchanged while only the composition of the water vapour in the layer is modified by the re-evaporating water molecules.

The main difference resulting from the two variants is that in case of the 3-D-ref variant the surface precipitation is composed like the near-surface water vapour, whereas in the case of the 3-D-mod variant the surface precipitation is composed like the water vapour that resides in those higher atmospheric layers where the precipitation originally formed. Consistent with what is common practice in atmospheric stable water isotope simulation studies (e.g. Hoffmann et al., 1998), one can argue that the 3-D-ref variant is a reasonable approximation for stratiform precipitation while the degree of mixing in the case of convective precipitation is somewhere between the two variants. However, we do not treat stratiform precipitation and convective precipitation (which are handled separately within ECHAM6) differently. Instead, we apply only one of the two variants at a time in separate simulations.

Simulations with the two variants 3-D-ref and 3-D-mod allow for us to estimate an upper bound for the uncertainty associated with the question of how strongly precipitation mixes on its way towards the surface with the ambient water vapour. The corresponding results are given in Appendix B. However, in the main part of the paper we consider only the 3-D-ref variant because (i) differences between the two variants are smaller than compared to the 2-D variant, and (ii) the 3-D-ref variant appears to be overall more realistic than the 3-D-mod variant (compare Hoffmann et al., 1998).

A3 2-D variant

One can convert the full 3-D tracing to a scheme that is equivalent to 2-D moisture tracing by imposing artificially well-mixed conditions (Sect. 2). This can be achieved by mixing completely the WVTs in each atmospheric column after every model time step while preserving the vertical profile of the total moisture, leading to the third tracing variant that we implemented, which is

$$\text{variant 2-D:} \quad q_i(z) = \hat{f}_i \cdot q(z)\,. \tag{A10}$$

Please note that it does not matter which of the 3-D variants is taken as a basis for the reduction to the 2-D variant because vertical differences in the WVT tendencies that exist between the two 3-D variants are immediately nullified by the application of Eq. (A10).

Appendix B

3-D-ref versus 3-D-mod

Here we discuss the uncertainties in 3-D moisture tracing arising from the different assumptions on how strongly precipitation mixes with the ambient water vapour. As described in Appendix A, we apply two variants of 3-D moisture tracing: in the case of the variant 3-D-ref, precipitation mixes instantaneously with the ambient water vapour, and in the case of the variant, 3-D-mod no mixing apart from that associated with net condensation/re-evaporation occurs. Since these variants are at the two extremes of the range of possible assumptions, they allow for us to estimate the maximum uncertainty associated with the question of how strongly precipitation mixes with the ambient water vapour.

Overall, the results obtained with the two 3-D tracing variants are less different from each other (Figs. B1 and B2) than compared to the results of 2-D tracing (Figs. 6e–f and 7e–f). This justifies that we considered only one of the 3-D variants, namely 3-D-ref, in the main part of this paper.

Differences between 3-D-ref and 3-D-mod are, however, not negligible. The most striking difference is that 3-D-mod almost exclusively gives lower values within the considered source regions (the continents/the three rectangular regions) and lower values outside. This pattern is reminiscent of the differences between 2-D and 3-D tracing, at least in the extratropics, and the explanation is again fast-recycling. While in the 3-D-ref variant the precipitation arriving at the surface reflects the composition of the near-surface atmospheric moisture, in the 3-D-mod variant the precipitation is composed like the moisture at those heights where it has formed (Appendix A). This implies that 3-D-mod features weaker fast-recycling than 3-D-ref. Given the vertically inhomogeneous distributions of local versus remote moisture (Figs. 4 and 5), this explains most of the differences between the results obtained with 3-D-mod and 3-D-ref.

The results for the evaporative sources of western Sahelian precipitation are very similar between 3-D-mod and 3-D-ref. This holds for the spatio-temporal pattern (not shown) as well as for the integrated amounts. Simulated with 3-D-mod, the contributions from N, SW, SE, and AFR are, respectively, 22 %, 26 %, 14 %, and 38 % (compare Table 2), corroborating the robustness of the comparison between 2-D and 3-D moisture tracing.

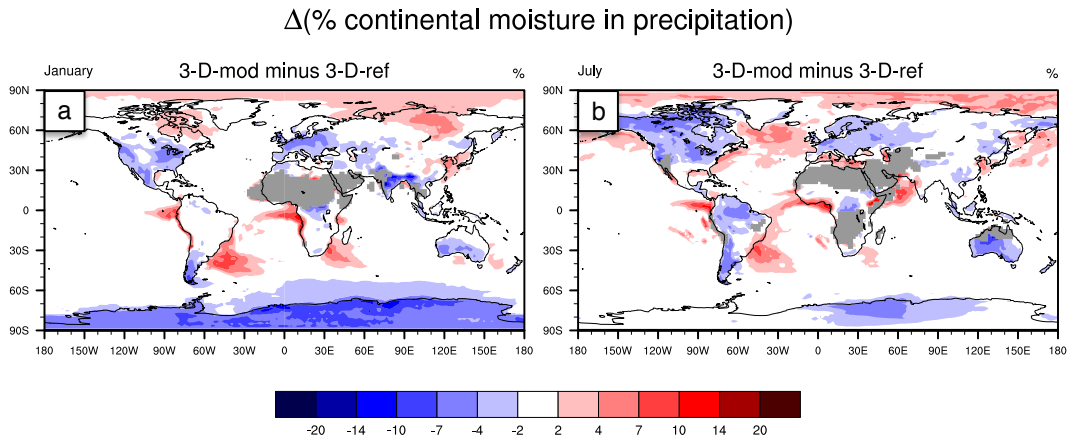

Fig. B1. The difference between the continental recycling ratios (R_C, % continental moisture in precipitation), as simulated with 3-D-ref and 3-D-mod, for January and July. Grey areas are masked because less than five out of the ten years used for computing the averages have non-zero precipitation in the considered month, leading to statistically non-robust estimates.

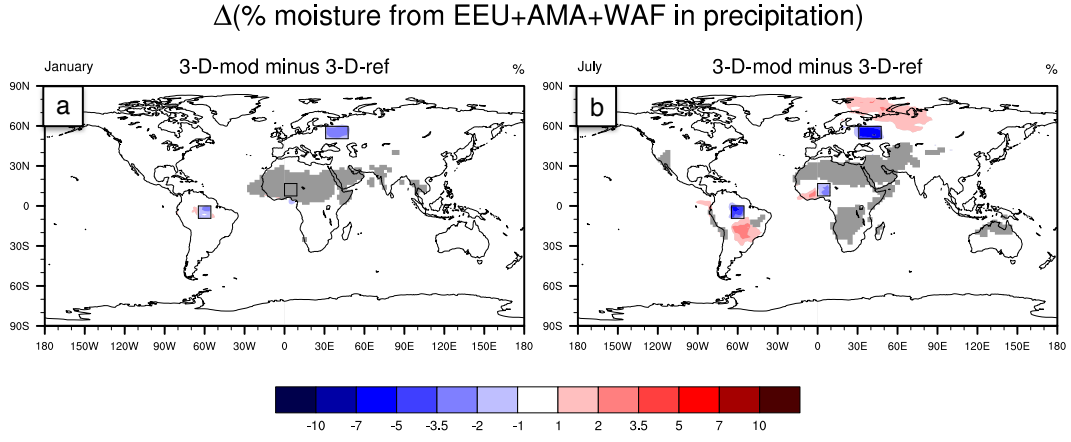

Fig. B2. The difference between the fraction of precipitation that originates from the rectangular source regions EEU, AMA, and WAF (black boxes), as simulated with 3-D-ref and 3-D-mod, for January and July. Grey areas are masked because less than five out of the ten years used for computing the averages have non-zero precipitation in the considered month, leading to statistically non-robust estimates.

Acknowledgements. We thank Veronika Gayler and Reiner Schnur for helping us to implement WVTs into ECHAM6. Sebastian Rast also supported us with the implementation and in addition gave valuable comments on the manuscript, for which we are very grateful. The simulations were carried out on the supercomputing system of the German Climate Computing Centre (DKRZ) in Hamburg. Most of the figures were generated with the NCAR Command Language (doi:10.5065/D6WD3XH5). We also thank the two reviewers R. van der Ent and H. Sodemann whose comments helped to improve the manuscript. Finally, HFG is indebted to Sebastian Bathiany for his invaluable comments on the global mean elevation of the continents.

The service charges for this open access publication have been covered by the Max Planck Society.

Edited by: F. Fierli

References

Bosilovich, M. G.: On the vertical distribution of local and remote sources of water for precipitation, Meteorol. Atmos. Phys., 80, 31–41, 2002.

Bosilovich, M. G. and Schubert, S. D.: Water vapor tracers as diagnostics of the regional hydrologic cycle, J. Hydrometeorol., 3, 149–165, 2002.

Bosilovich, M. G., Sud, Y., Schubert, S. D., and Walker, G. K.: GEWEX CSE sources of precipitation using GCM water vapor tracers, Global Energy and Water Cycle Experiment NEWS, 3, 6–7, 2002.

Brubaker, K. L., Entekhabi, D., and Eagleson, P. S.: Estimation of continental precipitation recycling, J. Climate, 6, 1077–1089, 1993.

Budyko, M. I.: Climate and Life, Int. Geophys. Ser. 18, Academic Press, New York and London, 1974.

Burde, G. I.: Bulk recycling models with incomplete vertical mixing. Part I: Conceptual framework and models, J. Climate, 19,

1461–1472, 2006.

Dansgaard, W.: Stable isotopes in precipitation, Tellus, 16, 436–468, 1964.

Dirmeyer, P.: Interactive comment on "Analyzing precipitationsheds to understand the vulnerability of rainfall dependent regions" by Keys et al., Biogeosciences Discuss., 8, C4544–C4546, 2011.

Dirmeyer, P. and Brubaker, K.: Contrasting evaporative moisture sources during the drought of 1988 and the flood of 1993, J. Geophys. Res., 104, p. 19383 doi:10.1029/1999JD900222, 1999.

Dominguez, F. and Kumar, P. and Liang, X. Z. and Ting, M.: Impact of Atmospheric Moisture Storage on Precipitation Recycling, J. Climate, 19, 1513–1530, doi:10.1175/JCLI3691.1, 2006.

Eltahir, E. A. B. and Bras, R. L.: Precipitation recycling in the Amazon basin, Q. J. Roy. Meteor. Soc., 120, 861–880, 1994.

Fitzmaurice, J. A.: A critical analysis of bulk precipitation recycling models, Ph. D. thesis, Massachusetts Institute of Technology, 2007.

Garratt, J.: The Atmospheric Boundary Layer, Cambridge University Press, Cambridge, 1992.

Gimeno, L., Stohl, A., Trigo, R. M., Dominguez, F., Yoshimura, K., Yu, L., Drumond, A., Duran-Quesada, A. M., and Nieto, R.: Oceanic and terrestrial sources of continental precipitation, Rev. Geophys., 50, RG4003, doi:10.1029/2012RG000389, 2012.

Goessling, H. F. and Reick, C. H.: What do moisture recycling estimates tell us? Exploring the extreme case of non-evaporating continents, Hydrol. Earth Syst. Sci., 15, 3217–3235, doi:10.5194/hess-15-3217-2011, 2011.

Hoffmann, G., Werner, M., and Heimann, M.: Water isotope module of the ECHAM atmospheric general circulation model: A study on timescales from days to several years, J. Geophys. Res., 103, 16871–16896, doi:10.1029/98JD00423, 1998.

Jöckel, P., von Kuhlmann, R., Lawrence, M., Steil, B., Brenninkmeijer, C., Crutzen, P., Rasch, P., and Eaton, B.: On a fundamental problem in implementing flux-form advection schemes for tracer transport in 3-dimensional general circulation and chemistry transport models, Q. J. Roy. Meteor. Soc., 127, 1035–1052, 2001.

Joussaume, S., Sadourny, R., and Vignal, C.: Origin of precipitating water in a numerical simulation of July climate, Ocean-Air Interact., 1, 43–56, 1986.

Keys, P. W., van der Ent, R. J., Gordon, L. J., Hoff, H., Nikoli, R., and Savenije, H. H. G.: Analyzing precipitationsheds to understand the vulnerability of rainfall dependent regions, Biogeosciences, 9, 733–746, doi:10.5194/bg-9-733-2012, 2012.

Koster, R., Jouzel, J., Suozzo, R., Russell, G., Broecker, W., Rind, D., and Eagleson, P.: Global sources of local precipitation as determined by the Nasa/Giss GCM, Geophys. Res. Lett., 13, 121–124, 1986.

Lettau, H., Lettau, K., and Molion, L. C. B.: Amazonia's hydrologic cycle and the role of atmospheric recycling in assessing deforestation effects, Mon. Weather Rev., 107, 227–238, 1979.

Lin, S.-J. and Rood, R.: Multidimensional flux-form semi-Lagrangian transport schemes, Mon. Weather Rev., 124, 2046–2070, 1996.

Möbis, B. and Stevens, B.: Factors controlling the position of the Intertropical Convergence Zone on an aquaplanet, J. Adv. Model. Earth Syst., 4, doi:10.1029/2012MS000199, 2012.

Nordeng, T.: Extended versions of the convection parametrization scheme at ECMWF and their impact upon the mean climate and transient activity of the model in the tropics, Tech. rep., Research Department Technical Memorandum, ECMWF, Reading, UK, 1994.

Numaguti, A.: Origin and recycling processes of precipitating water over the Eurasian continent: experiments using an atmospheric general circulation model, J. Geophys. Res., 104, 1957–1972, 1999.

Roeckner, E., Baeuml, G., Bonaventura, L., Brokopf, R., Esch, M., Giorgetta, M., Hagemann, S., Kirchner, I., Kornblueh, L., Manzini, E., Rhodin, A., Schlese, U., Schulweida, U., and Tompkins, A.: The atmospheric general circulation model ECHAM5. Part I: Model description, Tech. Rep. 349, Max Planck Institute for Meteorology, Hamburg, Germany, 2003.

Salati, E., Dall'Olio, A., Matsui, E., and Gat, J. R.: Recycling of water in the Amazon basin: an isotopic study, Water Resour. Res., 15, 1250–1258, 1979.

Sodemann, H., Wernli, H., and Schwierz, C.: Sources of water vapour contributing to the Elbe flood in August 2002 – a tagging study in a mesoscale model, Q. J. Roy. Meteor. Soc., 135, 205–223, 2009.

Stevens, B., Giorgetta, M. A., Esch, M., Mauritsen, T., Crueger, T., Rast, S., Salzmann, M., Schmidt, H., Bader, J., Block, K., Brokopf, R., Fast, I., Kinne, S., Kornblueh, L., Lohmann, U., Pincus, R., Reichler, T., and Roeckner, E.: Atmospheric component of the MPI-M Earth System Model: ECHAM6, J. Adv. Model. Earth Syst., 5, doi:10.1002/jame.20015, 2013.

Stohl, A. and James, P.: A Lagrangian analysis of the atmospheric branch of the global water cycle. Part I: Method description, validation, and demonstration for the August 2002 flooding in Central Europe, J. Hydrometeorol., 5, 656–678, 2004.

Tiedtke, M.: A comprehensive mass flux scheme for cumulus parameterization in large-scale models, Mon. Weather Rev., 117, 1779–1800, 1989.

van der Ent, R. J.: Interactive comment on "Atmospheric water vapour tracers and the significance of the vertical dimension" by Goessling and Reick, Atmos. Chem. Phys. Discuss., 12, C10180–C10188, 2012.

van der Ent, R. J. and Savenije, H. H. G.: Length and time scales of atmospheric moisture recycling, Atmos. Chem. Phys., 11, 1853–1863, doi:10.5194/acp-11-1853-2011, 2011.

van der Ent, R. J., Savenije, H. H. G., Schaefli, B., and Steele-Dunne, S. C.: Origin and fate of atmospheric moisture over continents, Water Resour. Res., 46, W09525, doi:10.1029/2010WR009127, 2010.

Yoshimura, K., Oki, T., Ohte, N., and Kanae, S.: Colored moisture analysis estimates of variations in 1998 Asian monsoon water sources, J. Meteorol. Soc. Jpn., 82, 1315–1329, 2004.